# High performance $Cu_2O$ film/ZnO nanowires self-powered photodetector by electrochemical deposition*

Deshuang Guo(郭德双), Wei Li(李微), Dengkui Wang(王登魁)†,
Bingheng Meng(孟兵恒), Dan Fang(房丹)‡, and Zhipeng Wei(魏志鹏)

*State Key Laboratory of High Powder Semiconductor Lasers, Changchun University of Science and Technology, Changchun* 130022, *China*

(Received 9 June 2020; revised manuscript received 2 July 2020; accepted manuscript online 15 July 2020)

Self-powered photodetectors based on nanomaterials have attracted lots of attention for several years due to their various advantages. In this paper, we report a high performance $Cu_2O$/ZnO self-powered photodetector fabricated by using electrochemical deposition. ZnO nanowires arrays grown on indium-tin-oxide glass are immersed in $Cu_2O$ film to construct type-II band structure. The $Cu_2O$/ZnO photodetector exhibits a responsivity of 0.288 mA/W at 596 nm without bias. Compared with $Cu_2O$ photoconductive detector, the responsivity of the $Cu_2O$/ZnO self-powered photodetector is enhanced by about two times at 2 V bias. It is attributed to the high power conversion efficiency and the efficient separation of the photogenerated electron–hole pairs, which are provided by the heterojunction. The outstanding comprehensive performances make the $Cu_2O$ film/ZnO nanowires self-powered photodetector have great potential applications.

**Keywords:** electrochemical deposition, $Cu_2O$/ZnO, self-powered photodetector, responsivity

**PACS:** 85.60.Dw, 73.40.Lq **DOI:** 10.1088/1674-1056/aba610

## 1. Introduction

Compared with photoconductive photodetectors, the photogenerated carriers are efficiently separated in self-powered photodetectors by built-in electric field, which enables detection without consuming external power. In addition, self-powered photodetectors possess the advantages of fast time response and high responsivity. Some researchers have fabricated self-powered photodetectors based on various structures, such as, Schottky junction,[1,2] p–n junction,[3,4] and photo electrochemical cell.[5] Although self-powered photodetectors have been developed for many years, their performances still cannot meet the requirement of commercially application at present.

In the past years, metal oxide semiconductors have been widely used in self-powered photodetectors due to their excellent photoconductivity and suitable bandgap.[6–8] Cuprous oxide ($Cu_2O$) is a natural p-type conductivity oxide semiconductor with bandgap of 2.1 eV,[9] which is an attractive material for photodetectors and solar cells owing to its high visible light absorption coefficient, superior theoretical conversion efficiency, and additional advantage of low cost.[10,11] The power conversion efficiency of ZnO/$Cu_2O$ solar cells is as high as 20% in theory.[12] At present, $TiO_2$,[13] ZnO,[15,16] and Si[17] nanostructures are used to build $Cu_2O$-based self-powered detectors. However, the performances of these $Cu_2O$-based photodetectors are still poor. The main reasons are bad crystalline quality of $Cu_2O$ and low separation of photogenerated carriers. The $Cu_2O$/ZnO heterojunctions have been used for various applications. However, limited charge transport characteristics impair the function of the final device. To enhance the performance of $Cu_2O$-based self-powered photodetectors, the qualities of the heterostructure need to be further improved. The structure of nanowires (NWs) immersed in $Cu_2O$ film provides large surface area and facilitates separation of photogenerated carriers, thereby improving the performance of the detector.

Because of the complicated preparation method and the unstable control of parameter ratio, the CuO often appears in $Cu_2O$ film,[18] which affects the photoelectric characteristics, increases the dark current, broadens the response peak, and reduces the responsivity. Moreover, the crystalline quality of $Cu_2O$ has great effect on the carrier separation efficiency, which limits the performance of the detector. Seeking for a method to fabricate high quality $Cu_2O$ films is urgent. Electrochemical deposition is a low-temperature, high-efficiency manufacturing method for high quality $Cu_2O$ nanostructure and film.[19]

In this paper, a $Cu_2O$/ZnO self-powered photodetector was prepared on indium-tin-oxide (ITO) glass substrate by electrochemical deposition. Its optical and electrical properties were studied in detail. A high responsivity of 0.288 mA/W at 596 nm without bias was obtained. The responsivity of the $Cu_2O$/ZnO self-powered photodetector was two times higher than that of $Cu_2O$ photoconductive detector at 2 V bias. This is because the separation efficiency of photogenerated electron–

*Project supported by the National Natural Science Foundation of China (Grant Nos. 61704011, 61674021, 11674038, 61574022, and 61904017) and the Innovation Foundation of Changchun University of Science and Technology (Grant No. XQNJJ-2018-18).

†Corresponding author. E-mail: wccwss@foxmail.com

‡Corresponding author. E-mail: fangdan19822011@163.com

 

hole pairs was greatly improved by introducing ZnO NWs.

## 2. Experimental data

In order to fabricate the self-powered photodetector, the ZnO NWs and the $Cu_2O$ film were grown by electrochemical deposition. First, ZnO NWs were prepared on ITO glass substrate ($< 10\ \Omega/cm^2$). An aqueous solution of 0.05 mol/L $Zn(NO_3)_26H_2O$ and $C_6H_{12}N_4$ was used as the precursor. ZnO NWs were deposited at 65 °C with voltage of −0.8 V for 30 min.[20] Then, the $Cu_2O$ film was deposited on ZnO NWs to form heterostructure. The precursor solution contained 3 mol/L lactic acid and 0.4 mol/L $CuSO_4$. Its pH was adjusted to 10 by adding NaOH. The $Cu_2O$ film was deposited at 60 °C with voltage of −0.6 V for 15 min.[21] The Au electrode was prepared on the $Cu_2O$ film by metal evaporation processes.

The surface morphology of the $Cu_2O$/ZnO heterojunction was characterized by scanning electron microscopy (SEM, Hitachi S-4800). The crystalline and structure were examined by x-ray diffractometer (XRD, Bruker D8-Focus). The optical properties were characterized by using UV–visible spectrophotometer (Shimadzu UV-2450). The current–voltage ($I$–$V$) curves were measured with a source meter unit (Keithley 2400). The photoresponse characteristics of the detector were tested by a spectral response system (Zolix DSR101UV-B).

## 3. Results and discussion

The morphology and the energy dispersive x-ray spectroscopy (EDS) of the $Cu_2O$ film are shown in Fig. 1(a). The compact $Cu_2O$ film is composed of cube structure with smooth surface, the average particle diameter is about 1.7 μm, and the particle distribution is uniform. The mole ratio of Cu and O is equal to 1.88, which is approximately consistent with stoichiometric ratio of $Cu_2O$. These results indicate that the $Cu_2O$ film possesses good quality. The diameter of ZnO NWs is 120 nm and the average length is about 2 μm, as shown in Fig. 1(b). The mole ratio of O and Zn is smaller than the stoichiometric ratio of ZnO, which is attributed to O vacancy or Zn interstitial atom. Cross section image of the $Cu_2O$/ZnO heterojunction presents that the ZnO NWs arrays penetrate inside $Cu_2O$ film, as shown in Fig. 1(c). The thickness of the heterojunction is about 6.0 μm. These SEM images show that the $Cu_2O$ has filled well into the gap between ZnO NWs, which effectively increases the contact area of the heterojunction and provides channels for carrier separation.

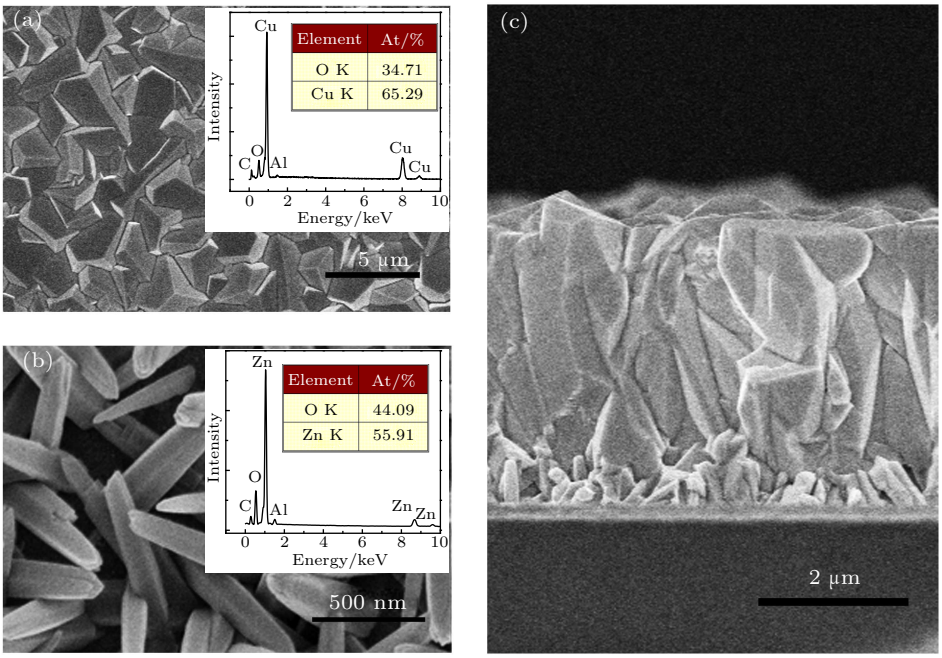


**Fig. 1.** (a) The SEM image and EDS of $Cu_2O$ film. (b) The SEM image and EDS of ZnO NWs. (c) The cross section SEM image of $Cu_2O$/ZnO heterojunction.

The crystal structures of the $Cu_2O$ film, ZnO NWs, and $Cu_2O$/ZnO heterojunction are studied by XRD techniques. As shown in Fig. 2(a), the diffraction peaks in the XRD pattern of the $Cu_2O$ film locate at 29.6°, 36.5°, 42.4°, and 61.5°, which are consistent with the (110), (111), (200), and (220) planes of cubic phase $Cu_2O$ (JCPDS 65-3288) [22]. The highest intensity corresponds to the (111) peak, suggesting the preferential growth orientation of $Cu_2O$ film with excellent crystalline quality. The XRD pattern of ZnO NWs possesses diffraction peaks at 31.6°, 34.3°, 36.2°, 56.5°, and 62.8°, which are attributed to the (100), (002) (101), (110), and (103) planes of hexagonal ZnO (JCPDS 36-1451) [23]. For the pattern of the $Cu_2O$/ZnO heterojunction, all diffraction peaks observed are consistent with $Cu_2O$ and ZnO. However, owing to the large

thickness of the $Cu_2O$ film, the peaks of ZnO NWs are weaker than those of $Cu_2O$.

The optical properties of the $Cu_2O$ film, ZnO NWs, and $Cu_2O$/ZnO heterojunction are characterized by absorption spectra, as shown in Fig. 2(b). It can be seen that there are two absorption edges in the absorption spectrum of the $Cu_2O$/ZnO heterojunction, which are 378 nm and 596 nm corresponding to absorption of ZnO and $Cu_2O$, respectively. The corresponding values of band gap are calculated according to the following equation:[24]

$$\alpha h\upsilon = \left(h\upsilon - E_g\right)^{1/2}, \tag{1}$$

where $\alpha$ is the absorption coefficient, $h\upsilon$ is the photon energy, and $E_g$ is the optical band gap. The values of $E_g$ are determined by extrapolations of the linear regions of the plots to zero absorption. The calculated band gap energies are 3.28 eV and 2.08 eV, which correspond to the band gaps of ZnO and $Cu_2O$, respectively.

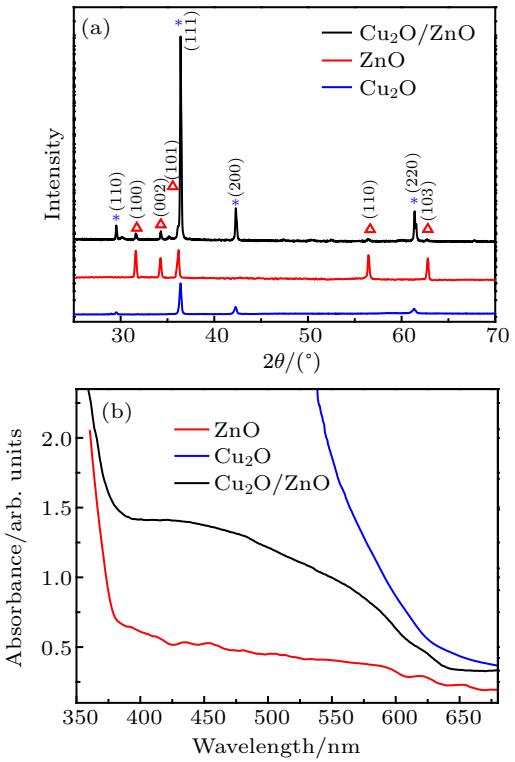


**Fig. 2.** (a) The XRD patterns and (b) UV–visible spectra of $Cu_2O$ film, ZnO NWs, and $Cu_2O$/ZnO heterojunction.

In order to understand the detection characteristics of $Cu_2O$/ZnO, we performed $I$–$V$ curves and spectral responsivity tests. Figure 3(a) shows the dark current and photocurrent profiles of $Cu_2O$ and $Cu_2O$/ZnO photodetector. The heterojunction exhibited $4.74\times10^{-4}$ A at 2 V bias, which is much higher than $2.73\times10^{-6}$ A of the $Cu_2O$ device under illumination. It can be seen from the insert of Fig. 3(a) that the photo $I$–$V$ curves of the $Cu_2O$/ZnO photodetector do not pass through the coordinate origin, which means that the device can work in self-powered mode without an external source. The responsivity spectrum of the $Cu_2O$/ZnO photodetector at 0 V bias is shown in Fig. 3(b). The detector shows a strong response peak of $2.88\times10^{-4}$ A/W at 596 nm. The performance of our device is much higher than that of the state-of-the-art $Cu_2O$-based photodetectors, as shown in Table 1.

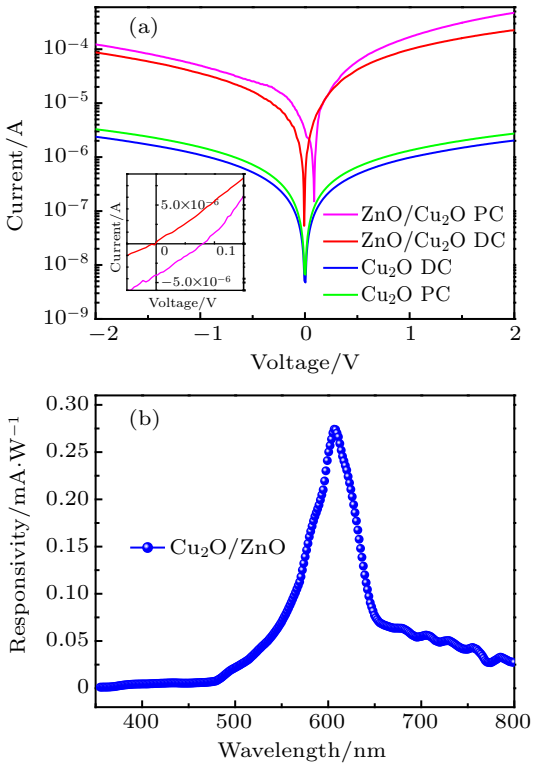


**Fig. 3.** (a) The $I$–$V$ curves of the $Cu_2O$ film and $Cu_2O$/ZnO heterojunction, the insert is a magnified image of $Cu_2O$/ZnO heterojunction near the origin. (b) Spectral responsivity of the $Cu_2O$/ZnO photodetector at 0 V bias.

**Table 1.** A comparison of the performances between this work and the state-of-the-art $Cu_2O$-based photodetectors.

| Materials | Wavelength/nm | Responsivity/(μA/W) | EQE/% | Ref. |
|---|---|---|---|---|
| ZnO/$Cu_2O$ films | | | 1.43 | [24] |
| $Cu_2O$ nanorods | | 8 | | [25] |
| $Cu_2O$ film-Au NPs | 532 | 23 | | [26] |
| $Cu_2O$/Cu | 590 | 300 | | [27] |
| Nanoscale ZnO/$Cu_2O$ films | | 280 | | [12] |
| ZnO/$Cu_2O$ core–shell NWs | | 7.67 | | [13] |
| AZO/ZnO/$Cu_2O$ films | | | 0.24 | [14] |
| $Cu_2O$ film/ZnO NWs | 596 | 288 | 2.4 | this work |

The energy band diagram of the heterojunction is plotted based on the analysis of absorption spectrum, as shown in Fig. 4. $\Delta E_c$ and $\Delta E_v$ represent the band offsets of the conduction band and valence band of ZnO and $Cu_2O$, respectively. The electron affinity of ZnO is 4.2 eV and that of $Cu_2O$ is 3.2 eV. When the p-$Cu_2O$ film contacts with n-ZnO, band bending occurs, and a built-in electric field is generated at the interface. Under light irradiation, a large number of electron–hole pairs are generated in the $Cu_2O$ film. Due to the type-II band structure, the electron–hole pairs are separated by the built-in electric field in the space charge region and collected at the electrode to generate current.[28,29] It indicates that the $Cu_2O$/ZnO heterojunction plays an important role on enhancing the photocurrent.

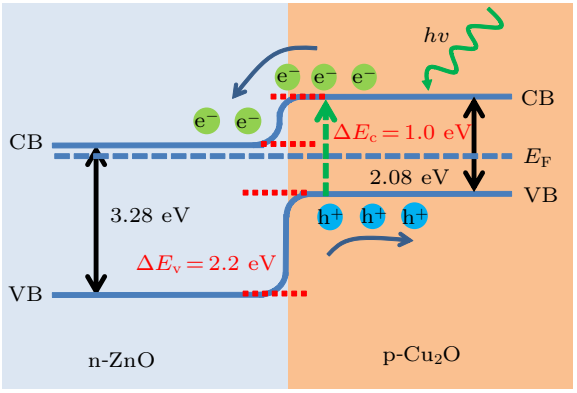


**Fig. 4.** Energy band diagram of $Cu_2O$/ZnO photodetector.

The response spectra of $Cu_2O$/ZnO self-powered photodetector and $Cu_2O$ photodetector at 2 V bias are shown in Fig. 5(a). The peak responsivity of the $Cu_2O$/ZnO photodetector was $1.15\times10^{-2}$ A/W at 596 nm, which was increased by 2.3 times than that of $Cu_2O$ photodetector ($4.95\times10^{-3}$ A/W). Compared with Figs. 2(b) and 5(a), although the photoabsorption of $Cu_2O$ film is better than that of $Cu_2O$/ZnO heterojunction, the responsivity of the $Cu_2O$ film photodetector is lower. It can be attributed to the type-II band structure of the $Cu_2O$/ZnO heterojunction, which improves the separation efficiency of the photogenerated electron–hole pairs. Furthermore, the ZnO NWs immersed in the $Cu_2O$ film increase the velocity of the photogenerated carriers at interface.

Besides the responsivity, external quantum efficiency (EQE) and detectivity ($D^*$) are main performance indicators of photodetectors. Considering the main source of noise, the $D^*$ and EQE can be expressed as[30–33]

$$D^* = \frac{A^{1/2}R}{(4K_0T/R_{\text{dark}} + 2eI_{\text{dark}})^{1/2}}, \tag{2}$$

$$EQE = \frac{Rhc}{\lambda e}, \tag{3}$$

where $R$ is the responsivity of the photodetector, $A$ is the effective detection area, $K$ is the Boltzmann constant, $T$ is the temperature, $R_{\text{dark}}$ and $I_{\text{dark}}$ are the resistance and current in dark, respectively, $h$ is Planck's constant, $c$ represents the velocity of light, $\lambda$ denotes the light wavelength, and $e$ is the electron charge. The $D^*$ of the $Cu_2O$/ZnO photodetector is $6.07\times10^8$ Jones under 2 V bias. According to Eq. (3), the EQE of the $Cu_2O$/ZnO photodetector is 2.4 %.

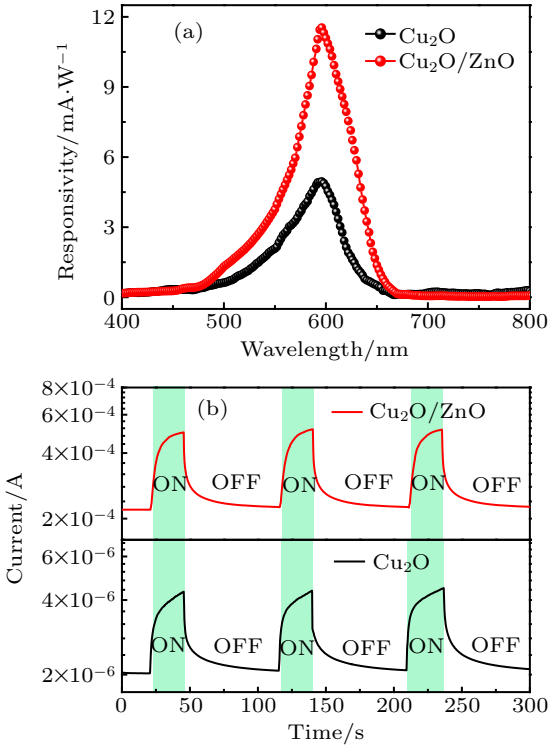


**Fig. 5.** (a) Spectral response of the $Cu_2O$/ZnO photodetector at 2 V bias. (b) The time-resolved current curves of $Cu_2O$/ZnO photodetector and $Cu_2O$ photodetector.

At last, the time-resolved currents were measured at 2 V to investigate the on–off performance of the $Cu_2O$ and $Cu_2O$/ZnO photodetectors, as shown in Fig. 5(b). The rise time (up to 90%) of the $Cu_2O$ photodetector and $Cu_2O$/ZnO photodetector is 17.7 s and 13.5 s, respectively. Meanwhile, the decay time (down to 10%) of the $Cu_2O$ photodetector and $Cu_2O$/ZnO photodetector is 21.9 s and 14.8 s, respectively. It can be seen that the rise time and the down time of the $Cu_2O$/ZnO photodetector are smaller than those of the $Cu_2O$ photodetector. This is because the type-II band structure increases the velocity of the photogenerated carriers at interface.

## 4. Conclusion

In summary, pure $Cu_2O$ film and ZnO NWs have been fabricated by electrochemical deposition. A self-powered photodetector with good performance has been realized by $Cu_2O$/ZnO heterojunction. The $Cu_2O$/ZnO self-powered photodetector shows excellent photoresponse performance (0.288 mA/W) at 596 nm without bias. Compare with $Cu_2O$ photoconductive photodetector, the responsivity of the $Cu_2O$/ZnO photodetector has great enhancement of 2.3 times

at 2 V bias, which is attributed to the improvement of separation efficiency by the $Cu_2O$/ZnO heterojunction.

## References


[1] Chen X, Liu K W, Zhang Z Z, Wang C R, Li B H, Zhao H F, Zhao D X and Shen D Z 2016 *ACS Appl. Mater. Inter.* **8** 4185

[2] Wu Y, Sun X J, Jia Y P and Li D B 2018 *Chin. Phys. B* **27** 126101

[3] Hatch S M, Briscoe J and Dunn S 2013 *Adv. Mater.* **25** 867

[4] Zhao Y, Wang N, Yu K, Zhang X M, Li X L, Zheng J, Xue C L, Cheng B L and Li C B 2019 *Chin. Phys. B* **28** 128501

[5] Bai B M and Zhang Y H 2016 *J. Alloy Compd.* **675** 325

[6] Wang P, Wang Y, Ye L, Wu M Z, Xie R Z, Wang X D, Chen X S, Fan Z Y, Wang J L and Hu W D 2018 *Small* **14** 1800492

[7] Zhou C Q, Ai Q, Chen X, Gao X H, Liu K W and Shen D Z 2019 *Chin. Phys. B* **28** 048503

[8] Wang Y, Wang P, Zhu Y K, Gao J R, Gong F, Li Q, Xie R Z, Wu F, Wang D, Yang J H, Fan Z Y, Wang X Y and Hu W D 2019 *Appl. Phys. Lett.* **114** 011103

[9] Messaoudi O, Makhlouf H, Souissi A, Assakeret I B, Amiri G, Bardaoui A, Oueslati M, Bechelany M and Chtourou R 2015 *Appl. Surf. Sci.* **343** 148

[10] Zhou T W, Zang Z G, Wei J, Zheng J F, Hao J Y, Ling F L, Tang X S, Fang L and Zhou M 2018 *Nano Energy* **50** 118

[11] Liao L, Yan B, Hao Y F, Xing G Z, Liu J P, Zhao B C, Shen Z X, Wu T, Wang L, Thong J, Li C M, Huang W and Yu T 2009 *Appl. Phys. Lett.* **94** 113106

[12] Minami T, Nishi Y and Miyata T 2016 *Appl. Phys. Express* **9** 052301

[13] Tsai T Y, Chang S J, Hsueh T J, Hsueh H T, Weng W Y, Hsu C L and Dai B T 2011 *Nanoscale Res. Lett.* **6** 575

[14] De Melo C, Jullien M, Battie Y, Naciri A E, Ghanbaja J, Montaigne F, Pierson J F, Rigoni F, Almqvist N, Vomiero A, Migot S, Mucklich F and Horwat D 2019 *ACS Appl. Nano Mater.* **2** 4358

[15] Ghamgosar P, Rigoni F, You S, Dobryden I, Kohan M G, Pellegrino A L, Concina I, Almqvist N, Malandrino G and Vomiero A 2018 *Nano Energy* **51** 308

[16] Noda S, Shima H and Akinaga H 2013 *J. Phys.: Conf. Ser.* **433** 012027

[17] Kim H, Kim S H, Ko K Y, Kim H, Kim J, Oh J and Lee H 2016 *Electron. Mater. Lett.* **12** 404

[18] Reddy M H P, Sreedhar A and Uthanna S 2011 *Indian J. Phys.* **86** 291

[19] Fujimoto K, Oku T and Akiyama T 2013 *Appl. Phys. Express* **6** 086503

[20] Dalvand R, Mahmud S and Rouhi J 2015 *Mater. Lett.* **160** 444

[21] Wu L, Tsui L, Swami N and Zangari G 2010 *J. Phys. Chem. C* **114** 11551

[22] Zou X, Fan H, Tian Y and Yan S 2014 *CrystEngcomm* **16** 1149

[23] Sun Y, Fox N A, Fuge G M and Ashfold M 2010 *J. Phys. Chem. C* **114** 21338

[24] Lu H C, Chu C L, Lai C Y and Wang Y H 2009 *Thin Solid Films* **517** 4408

[25] Wang R C and Li C H 2012 *J. Electrochem. Soc.* **159** K73

[26] Jia R, Lin G, Zhao D, Zhang Q, Lin X, Gao N and Liu D 2015 *Appl. Surf. Sci.* **332** 340

[27] Elfadill N G, Hashim M R, Saron K M A, Chahrour K M, Qaeed M A and Bououdina M 2015 *Mater. Chem. Phys.* **156** 54

[28] Wu F, Li Q, Wang P, Xia H, Wang Z, Wang Y, Luo M, Chen L, Chen F S, Miao J S, Chen X S, Lu W, Shan C X, Pan A L, Wu X, Ren C W, Jariwala D and Hu W D 2019 *Nat. Commun.* **10** 4663

[29] Tang Y, Cai Q, Yang L H, Dong K X, Chen D J, Lu H, Zhang R, Zheng Y D 2017 *Chin. Phys. Lett.* **34** 018502

[30] Li W, Wang D K, Zhang Z Z, Chu X Y, Fang X, Wang X W, Fang D, Lin F Y, Wang X H and Wei Z P 2018 *Opt. Mater. Express* **8** 3561

[31] Liu X, Gu L L, Zhang Q P, Wu J Y, Long Y Z and Fan Z Y 2014 *Nat. Commun.* **5** 4007

[32] Wu J M and Chang W E 2014 *ACS Appl. Mater. Inter.* **6** 14286

[33] Sun J M, Peng M, Zhang Y S, Zhang L, Peng R, Miao C C, Liu D, Han M M, Feng R F, Ma Y D, Dai Y, He L B, Shan C X, Pan A L, Hu W D and Yang Z X 2019 *Nano Lett.* **19** 5920